Innovative applications and behaviour of composite slabs with deep trapezoidal sheeting

M. A. Bradford, F. M. Abas, A. Gholamhoseini, R. I. Gilbert, S. J. Foster and Z.-T. Chang

Centre for Infrastructure Engineering, School of Civil and Environmental Engineering, The University of New South Wales, UNSW Sydney, 2052, Australia (Email: m.bradford@unsw.edu.au; fairul@unsw.edu.au; a.gholamhoseini@unsw.edu.au; i.gilbert@unsw.edu.au; s.foster@unsw.edu.au; z.chang@unsw.edu.au)

ABSTRACT

Technologies using composite slabs with profiled steel decking are a mature application of steel-concrete composite construction in steel-framed buildings. In Australia, thin-walled steel decks have traditionally been of a re-entrant type, and only recently have deep trapezoidal steel decks found application in composite flooring systems. This paper considers on-going research at The University of New South Wales on two issues related to the use of trapezoidal sheeting when the shear connection relevant to the behaviour is in the direction of the decking ribs. The first considers the restraint against drying shrinkage of the concrete, which results in potential shrinkage-warping deflections because the egress of moisture during drying is prevented at the soffit of the slab, but is free to occur at the top of the slab. There is no guidance on this aspect of structural design in either AS3600 or AS2327, and practitioners have been seeking solutions for some time. The second issue is that of using steel-fibre reinforced concrete slabs with trapezoidal sheeting in continuous slab construction, as would occur over a secondary beam in a flooring system. Based on tests, it is shown that this application has significant promise as a replacement for reinforcing mesh or bars that have to be placed on-site using manual techniques.

KEYWORDS

Composite slabs; Steel fibre reinforced concrete; Creep; Shrinkage; Partial interaction; Cracking.

INTRODUCTION

The synergies between the steel and concrete in composite beams and slabs are widely-known in structural design (Oehlers and Bradford, 1995). In steel-framed buildings (Fig. 1), the shear connection is in two directions: along the secondary beam where it is achieved by headed stud connectors located in the troughs of the decking, and along the ribs in the sheeting orthogonal to the steel ribs where it is achieved through friction, adhesion and aggregate interlock. Most research in this common application has concerned the strength issue with stud connectors in troughs (Bradford *et al.*, 2006; Ranzi *et al.*, 2009). On the other hand, the shear connection along the ribs poses significant challenges in structural modelling. In particular, it is of relevance for concrete slabs in which trapezoidal decking is used as “sacrificial” formwork, and slabs that are continuous over secondary beams for which hogging bending exists over the internal support. These two applications are considered in the current paper.

Using steel decking either in lieu of plywood forms, or to achieve large spans between secondary beams in steel framed buildings, requires not only the short-term composite action to be considered, but also the effect on deflections and stresses caused by shrinkage warping. This effect occurs because the steel decking both restrains the concrete and produces a gradient of shrinkage through the slab depth since its imperviousness retards the egress of moisture during drying shrinkage.

Hitherto, surprisingly little research has addressed this effect, both theoretically and experimentally, despite the frequent use of composite slabs and those with deep trapezoidal profiles in particular.

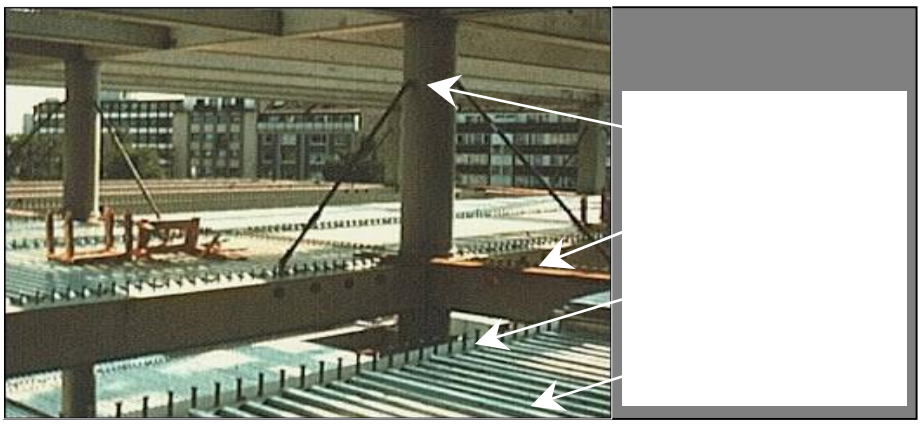

Figure 1. Composite building frame showing steel beams and columns, headed stud connectors and decking.

In continuous slabs, the hogging region over an internal support is conventionally reinforced with steel fabric and/or bars. However, the on-site fixing can be costly and maintaining the correct location of the reinforcing can be problematic and, despite its added expense, the use of steel-fibre reinforced concrete (SFRC) as a replacement for plain concrete with conventional reinforcing is a potential design solution, especially when deep trapezoidal decking whose top flanges are in the tensile zone of the concrete is used.

This paper reports on current research being undertaken at The University of New South Wales on: (i) the service-load response of simply-supported composite slabs with plain concrete, and (ii) the short-term response of continuous slabs with SFRC. Both of these research endeavours and outcomes will lead to much-needed guidance in the industry, particularly as carbon taxing dictates the optimum use of construction materials.

SHRINKAGE DEFORMATIONS OF SIMPLY-SUPPORTED SLABS

Experimental program

The shrinkage-induced strain distributions through the thickness of composite slab specimens were measured in the slab for a period of 322 days. Each specimen was 750 mm square in-plan, being moist cured for 21 days prior to the commencement of drying. The mean concrete compressive strength at 28 days was 34·5 MPa and the mean shrinkage strains measured on 75×75×280 mm companion prisms after 56 and 322 days of drying were -520×10^{-6} and -608×10^{-6} respectively. Two specimens (A and B) were constructed and monitored; the ‘A’ specimens being restrained with the steel decking in place as permanent formwork and providing restraint to drying shrinkage while the ‘B’ specimens were unrestrained, with no decking in place during drying and therefore no restraint to shrinkage. The ‘B’ specimens were created using polystyrene moulds fabricated to the same profile as the steel decking and, on removal, the soffit was coated with an impermeable flexible sealant to eliminate drying shrinkage from that surface. The concrete side faces of the specimens were also sealed. Specimens 1A and 1B were 150 mm thick with Fielders KingFlor® KF40 decking, 2A and 2B were 150 mm thick with KF70 decking, 3A and 3B were 200 mm thick with K70 decking and 4A and 4B were 300 mm thick with KF70 decking.

For each specimen, the concrete strains were measured using vibrating wire strain gauges embedded in the concrete at various depths through the thickness, and a Demec gauge was used to measure the concrete strains on the top and bottom surfaces of the slabs. For the restrained slabs, strain gauges attached to the steel decking at various locations also recorded the steel strains that developed as a result of restraint. Fig. 2 shows typical specimens, which were mounted vertically to allow for easy access. The specimens were supported on round steel bars to eliminate friction with the laboratory floor and were stabilised with a wooden frame.

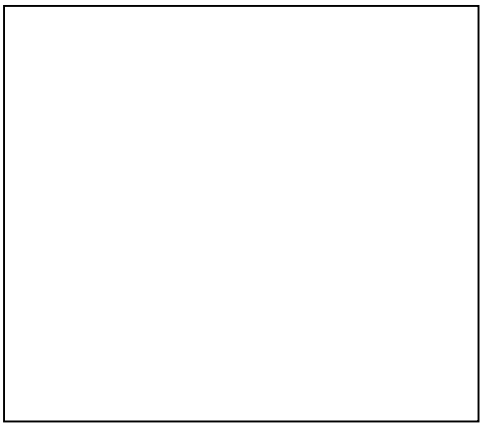

Figure 2. Shrinkage profile specimens (type 'A' in foreground and type 'B' in background).

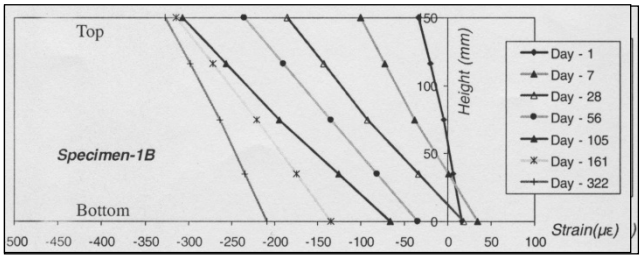

Figure 3. Strain profiles through 150 mm thick slab with KF40 deck profile.

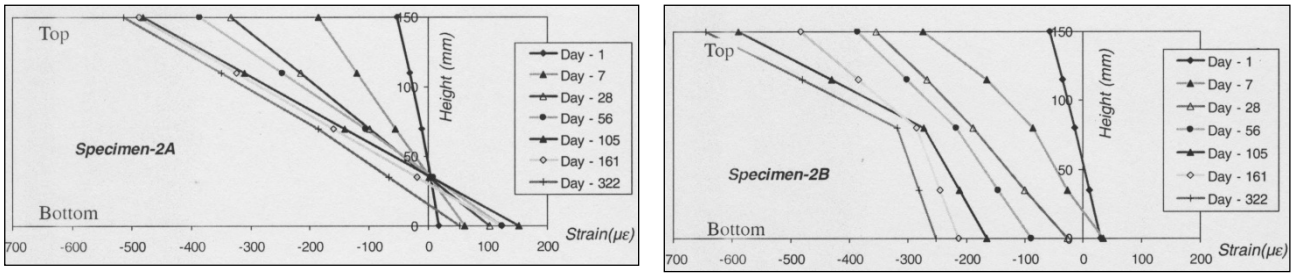

Figure 4. Strain profiles through 150 mm thick slab with KF70 deck profile.

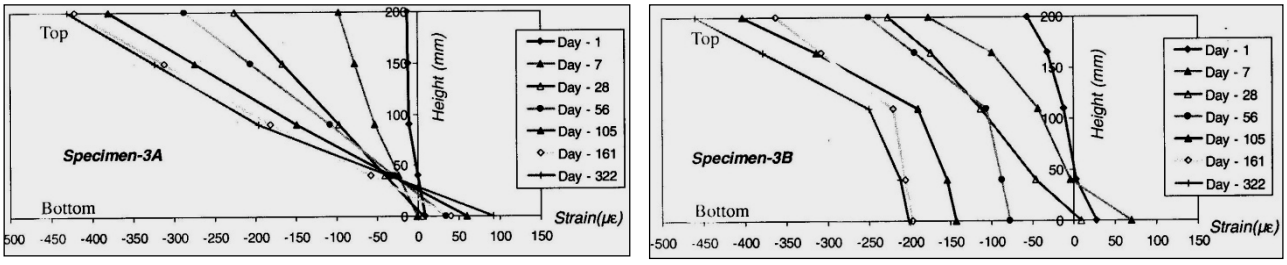

Figure 5. Strain profiles through 200 mm thick slab with KF70 deck profile.

The measured strain profiles in the two 150 mm thick slab specimens with KF40 trapezoidal decking are shown in Fig. 3. The strain in 1A is the total strain, which includes shrinkage strain plus the elastic and creep strains that developed with time due to the restraint to shrinkage provided by the steel decking. The strain measured in 1B is the shrinkage strain and, with no restraint from any steel decking, the elastic and creep strains will be small (the measured strain may include elastic and creep strains caused by the eigenstresses that could develop in the actual shrinkage strain profile was non-linear).

It appears that the sealing compound on the bottom of the specimens did not completely eliminate the drying shrinkage, as significant strain was measured in the bottom fibres after about 1 month of drying. While some of this strain may be due to autogenous shrinkage, it is more likely to be caused by drying as the bulk of the autogenous shrinkage tends to occur in the first two or three weeks after setting. A comparison of the strain distributions in 1A and 1B shows that significant restraint was provided by the steel decking. For example, the bottom fibre strains in 1A and 1B after 322 days of drying were -87×10^{-6} and -208×10^{-6}. The counterpart top fibre strains were -367×10^{-6} and -327×10^{-6}. The difference between these two strain profiles represents the strain caused by the tensile retraining force exerted by the steel decking of $+121\times10^{-6}$ at the bottom fibre and -40×10^{-6} at the top fibre.

Fig. 4 shows the measured strain profiles in two 150 mm thick slabs with the deeper KF70 trapezoidal decking profile, while Fig. 5 shows the strain profiles for 200 mm thick slabs with KF70 decking. It can be seen that the unrestrained specimens have close to bi-linear distributions of strains.

Theoretical analysis

Models that include shrinkage gradients, creep and partial interaction are difficult to formulate; one such treatment was presented by Bradford (2010), which produces a solution in analytical form but which assumes that the concrete does not crack. With the assumption of full interaction, a cross-sectional analysis may be formulated as described by Gilbert *et al.* (2012), which uses a layered cross-section to allow for the variation of the shrinkage strains and the possibility of cracking.

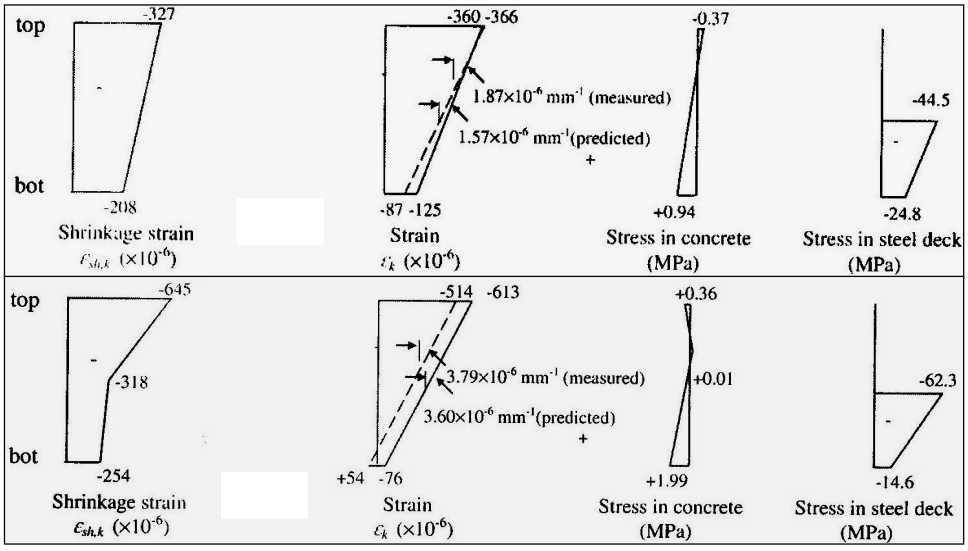

Figure 6. Measured strains versus predicted strains, and predicted stresses.

Comparison of experiments and theory

A 150 mm thick slab with KF40 and KF70 profiles has been analysed (deck thickness = 0·75 mm), being unloaded and subjected to the measured shrinkage strain profile measured at 322 days on the corresponding unrestrained specimen (1B and 2B respectively). The short-term elastic modulus was

29·6 GPa, tensile strength = 3·5 MPa, creep coefficient = 2·5, aging coefficient = 0·65, shrinkage strain at top surface = -645×10^{-6} and elastic modulus of the deck = 200 GPa. The stresses and deformations predicted by the analytical procedure are shown in Fig. 6. Considering the large variability in shrinkage measurements in seemingly identical control specimens, the predicted strain distributions are in good agreement with the measured distributions and the curvatures are in excellent agreement with the measured values. In addition, the predicted concrete stress at the bottom of each slab is significant (almost 60% of the flexural tensile strength of the concrete in Fig. 6b), indicating the very significant reduction in the cracking moment that is caused by shrinkage in these slabs.

STRENGTH OF SFRC CONTINUOUS SLABS

Two span continuous composite slabs fabricated using Lysaght W-dek® trapezoidal steel sheeting and steel fibre reinforced concrete were cast and loaded to failure in order to investigate the behaviour and characteristics of composite slabs containing steel fibres with and without conventional reinforcement in the hogging bending region. The slab specimens were constructed from a ready-mix concrete containing various dosages of steel fibres ranging from 0 kg/m^3 to 40 kg/m^3 by volume of high strength steel, end hooked fibres (Dramix RC80/60 BN and RC65/35BN). In total 8 prismatic SFRC composite slabs with deep trapezoidal decking were cast and moist cured for a period of 28 days. A schematic diagram of the slabs and supports is shown in Fig. 7. The concrete properties were measured on companion specimens in the form of standard cylinders and prisms for every batch of concrete. For each specimen the deflection of each span, the crack widths over the interior support and slip between the decking and the concrete at both ends of the slab were recorded electronically at each load increment from zero up to the failure of the specimen. Also recorded continuously throughout the tests were the applied loads and the reactions at the supports.

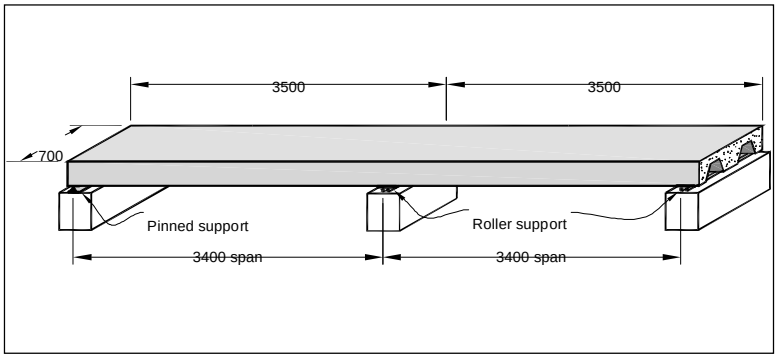

Figure 7. Dimensions and geometry of SFRC two-span composite slab test specimens

Because the aim of the testing program was to investigate the effectiveness of steel fibres as reinforcement in the negative moment region of continuous composite slabs in terms of both strength and serviceability, the test specimens comprised of the following four types:

- Slab without any steel fibres and without any conventional reinforcement (one specimen);
- Slab without any steel fibres, but with welded-wire mesh as top reinforcement over the internal support (one specimen);
- Slabs with steel fibres, but without any conventional reinforcement (four specimens); and
- Slabs reinforced without steel fibres and welded-wire mesh as top reinforcement (two specimens).

Details of the test specimens are given in Table 1. For the specimen identifier, the first term is the specimen number (S1 to S8), the second term is the nominal fibre dosage (kg/m^3) and fibre type (L for 60 mm, S for 35 mm) and the third term represents the type of mesh (wire size and spacing). All specimens were cast on W-dek sheeting that was 7000 mm long, 700 mm wide and 140 mm deep. Headed stud connectors (19 mm diameter) were welded through the W-dek at mid-length into a 6 mm

thick steel plate, in order to replicate a steel beam in two-way composite flooring systems as well as to initiate mid-span cracking. Fig. 8 shows schematically the instrumentation set-up for all slabs. The reactions at each support were measured using load cells, while linear varying displacement transducers (LVDTs) were used to measure the slip between the concrete and decking at each end (except for Specimen S9-60-00 which used dial gauges). Strains were measured at the internal supports and at the middle of each span, and the crack widths at mid-length were measured physically using a microscope.

Table 1. Details of test specimens

Specimen ID	Fibre length (mm)	Nominal fibre dosage (kg/m^3)	Measured fibre dosage by vol. (kg/m^3)	% by weight	Mesh size and reinforcement ratio
S1-0-00	-	-	-	-	-
S2-0-F62	-	-	-	-	F62 (0·2%)
S3-20-00	60	20	18·76	0·24	-
S4-30-00	60	30	27·92	0·36	-
S5-30-F52	60	30	30·57	0·39	F52 (0·1%)
S6-30-F82	60	30	27·92	0·36	F82 (0·26%)
S7-40-00	60	40	38·27	0·49	-
S8-40(S)-00	35	40	40·21	0·51	-
S9-60-00	60	60	59·86	0·76	-

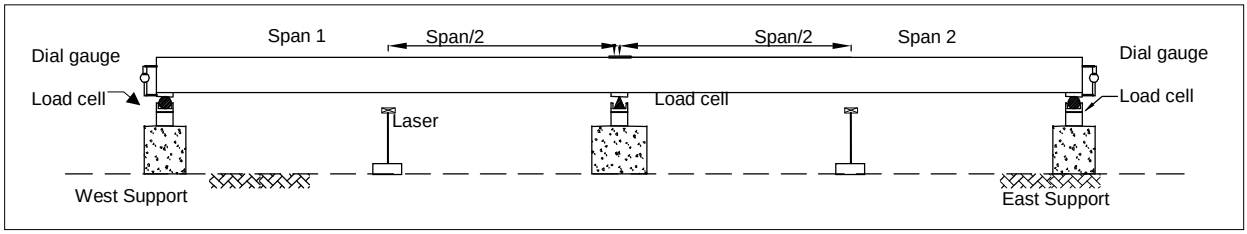

Figure 8. Schematic details of loading and instrumentation.

Table 2. Slab material properties.

Specimen #	$f_{c,ave}$ (MPa)	E_{conc} (GPa)	f_t (direct) (MPa)	f_t (flexural) (MPa)	G_f (N·m)
S1	49·1	30·1	3·65	4·44	129
S2	46·3	29·1	4·52	4·59	189
S3	43·5	27·5	3·55	3·90	3,470
S4	45·5	27·4	4·75	5·05	7,410
S5	45·0	30·4	3·33	5·06	4,260
S6	45·5	27·4	4·75	5·05	7,410
S7	42·8	33·1	2·73	4·62	5,520
S8	57·8	31·7	3·93	5·15	3,250
S9	49·0	27·5	4·28	8·27	19,190

The loading was applied with a spreader beam using a displacement-controlled actuator, with deformation being applied slowly and continuously for each specimen to capture the pre and post-peak response, with the test terminating when a drop below the peak load in excess of 30% occurred. Table 2 shows the material properties measured for the slab, in which $f_{c,\text{ave}}$ = average compressive strength, E_{conc} = elastic modulus of the slab, f_t = tensile strength and G_f = fracture energy. The sheeting had a mean elastic modulus of 192 GPa and a mean 0·2% offset stress of 685 MPa. The results from the slab tests are summarised in Table 3, in which P_{cr} = load to cause first cracking of the slab at its mid-span, P_{sl} = load at which slip commenced at the steel-concrete interface at the ends of the slab, P_{ult} = peak load for the slab, and in which $\delta_{s,ult}$ = slip deflection measured at the ultimate load at the ends of the slab and $\delta_{v,ult}$ = transverse deflection measured at the middle of the spans.

Table 3. Numerical test results.

Specimen #	P_{cr} (kN)	P_{sl} (kN)	P_{ult} (kN)	$\delta_{s,ult}$ (mm)	$\delta_{v,ult}$ (mm)
S1	25	37	62	7·6	51
S2	14	55	70	3·5	33
S3	20	60	93	7·0	49
S4	20	62	93	6·5	56
S5	32	67	89	7·6	53
S6	15	79	99	4·9	41
S7	12	57	83	5·1	43
S8	15	82	96	5·3	45
S9	25	69	88	-	39

A typical load-slip curve is shown in Fig. 9 for Specimen S4-30-00. Prior to attaining the load P_{sl} (62 kN in this case), the slip deflections at the end of the beam were negligible, and once slip commenced the mid-span flexural crack started to grow. Sensibly, this load can be considered as that at which the shear connection strength is reached under a condition of partial shear connection (Oehlers and Bradford, 1995). The ensuring behaviour was strain hardening under deformation control, and is typical for all slabs tested, including that without conventional and fibre reinforcement (S1-00-00). Some slabs were found to behave as shown for S7-40-00 in Fig. 5, when the breaking of the mechanical bond between the slab and sheeting was accompanied by a drop in load as the shear connection reached its capacity. All load-transverse deflection curves showed considerable ductility; those for S1-00-00 and S7-40-00 are shown in Fig. 10. Fig. 11 illustrates the ductile response of S3-20-00 at failure.

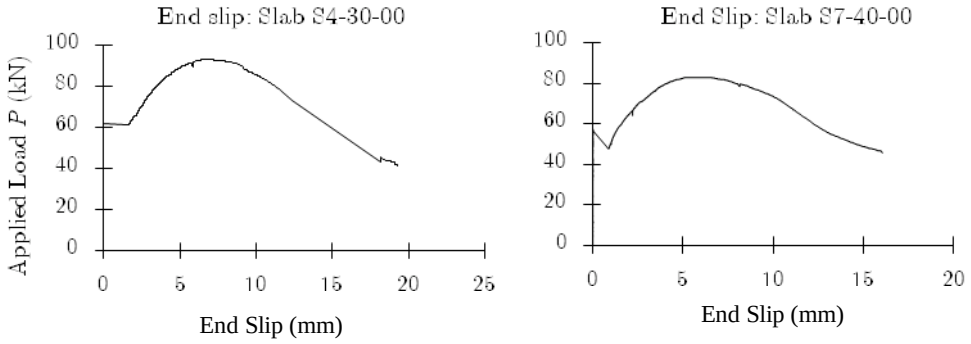

Load-slip responses (Sl

The evolution of cracking in the slabs with load increments is an important characteristic of the slabs for the serviceability limit state, and Fig. 12 shows this development for Specimens S1-00-00 and S7-40-00. The summary for all specimens is given in Table 4, where the equivalent imposed load to cause first cracking and that to cause a 0·3 mm wide crack are tabulated. The equivalent load was determined from the bending moments in the slab, obtained from force statics using the loads measured in the load cells.

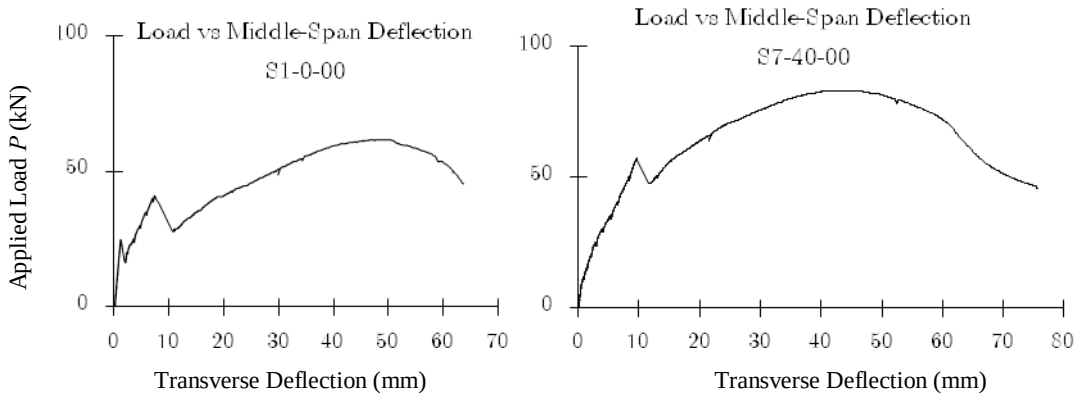

ıd-transverse defl

Figure 11. Photograph at failure of slab S3-20-00

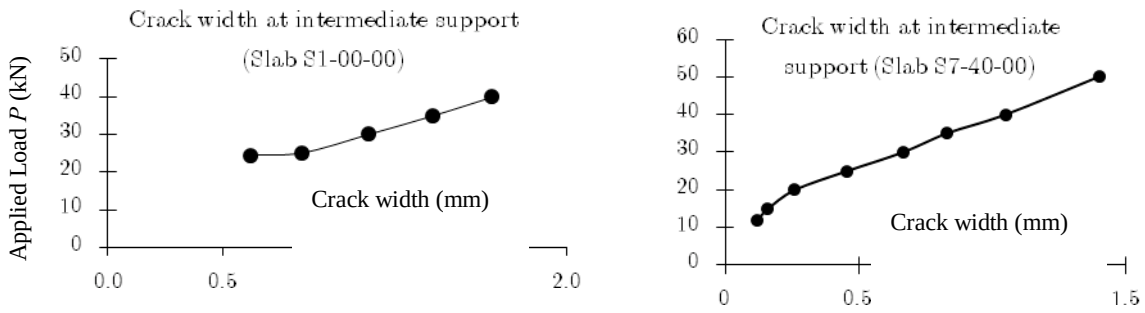

Figure of crack widths at internal

Table 4: Loads for serviceability limits.

Specimen #	First crack width (mm)	Imposed load at first crack (kPa)	Imposed load at 0.3 mm crack (mm)
S1	0·62	8·28	-
S2	0·16	5·47	8·56
S3	0·06	7·16	8·28
S4	0·17	7·16	8·28
S5	0·22	10·52	12·20
S6	0·06	5·76	16·97
S7	0·12	4·91	7·72
S8	0·16	5·76	6·60
S9	0·13	8·22	9·64

OBSERVATIONS AND CONCLUSIONS

This paper has presented studies of composite slabs with deep trapezoidal steel decks. With regard to shrinkage-induced deformations, which currently are not covered in Australian codes of practice, test results have been presented to allow empirical formulations of the shrinkage strain profile through the thickness of the slab. A theoretical analysis, using a layered cross-sectional approach, was shown produce deflections that agree with those measured in the tests and this procedure will form the basis for formulating design guidance.

With regard to the continuous composite slabs using SFRC, it was found that:

- Compared to the slab containing SL62 mesh over the interior support, the slab containing only 20 kg/m^3 of 65 mm long end-hooked steel fibres had a higher slip load and a higher peak load. In addition, the deflection at both the peak load and the slip load was greater for the slab containing fibres.
- The addition of 20 kg/m^3 of 65 mm long end-hooked steel fibres increased the slip load by about 59%, i.e. from P = 41 kN (for S1-0-00) to P = 65 kN (for S3-20L-00).
- The addition of 20 kg/m3 of 65 mm long end-hooked steel fibres increased the peak load by 34%, i.e. from P = 61.8 kN (for S1-0-00) to P = 82.8 kN (for S3-20L-00).
- The inclusion of steel fibres increases the ratio of slip load to peak load, from 63% (for S1-0-00) to 75% (for S3-20L-00).
- In terms of both the slip load and the peak load, relatively little benefit was gained by increasing the fibre content above 20 kg/m^3. The current practice of providing SL62 mesh over the negative moment region provided crack control (maximum crack widths of 0.3 mm) up to about 50% of the slip load. The same was true for the slabs containing only fibres. However, at loads above 50% of the slip load, the mesh was more effective at limiting the maximum crack width. Crack control was most effective for the slabs containing both mesh and fibres.
- In terms of maximum crack widths, relatively little benefit was gained by increasing the fibre content above 20 kg/m3.
- The use of 35 mm long fibres (Dramix RC65/35BN), compared to a similar volume of 60 mm long fibres (Dramix RC80/60 BN), increased both the slip load and the peak load, but had little effect on the maximum crack width at similar load levels.
- The inclusion of steel fibres (as an alternative to the use of SL62 mesh over the interior supports) is an effective measure to increase both the slip load and the peak load of continuous composite

slabs. Under typical service loads, cracking over the interior support will be controlled for most applications.

- Where a strong degree of crack control is required for the top surface of the slab, an effective measure to gain the benefits of fibres without the use of reinforcing mesh, is to use a saw-cut over the interior support. This will ensure the top crack occurs directly under the saw cut and is effectively hidden from view. In this way, the benefits of fibres in increasing the slip load and the peak load are gained, and the problems of crack control are eliminated.

ACKNOWLEDGEMENTS

The work in this paper was supported by the Australian Research Council through Linkage Projects LP0991701 and LP0991499. The support of partner organisations Fielders Australia, Prestressed Concrete Consultants Pty Ltd, BOSFA and BlueScope Lysaght Pty Ltd is acknowledged.

REFERENCES

Bradford M. A. (2010). Generic modelling of composite steel-concrete slabs subjected to shrinkage, creep and thermal strains including partial interaction. *Engineering Structures*, **32**(5), 1459-1465.

Bradford M. A., Filonov A., Hogan T. J., Uy B. and Ranzi G. (2006). Strength and ductility of shear connection in composite T-beams with trapezoidal steel decking. *8th Int. Conf. on Steel, Space and Composite Structures*, Kuala Lumpur, Malaysia, pp. 15-26.

Gilbert R. I., Bradford M. A., Gholamhoseini A. and Chang Z.-T. (2012). Effects of shrinkage on the long-term stresses and deformations of composite concrete slabs. *Engineering Structures*, **40**, 9-19.

Oehlers D. J. and Bradford M. A. (1995). *Composite Steel and Concrete Structural Members: Fundamental Behaviour*. Pergamon, Oxford.

Ranzi G., Bradford M. A., Ansourian P., Filonov A, Rasmussen K. J. R., Hogan T. J. and Uy B. (2009). Fill-scale tests on composite steel-concrete beams with trapezoidal decking. *Journal of Constructional Steel Research*, **65**(7), 1490-1506.